文章编号：1001－9014(2018)01－0025－05

DOI:10.11972/j.issn.1001－9014.2018.01.006

The photoelectric property of graphene modified by boron and nitrogen atoms from density functional theory calculation

LI Jia-Bin, LIU Hong-Xia*, WU Lei

(Key Laboratory for Wide Band Gap Semiconductor Materials and Devices of Education, School of Microelectronics, Xidian University, Xi'an 710071, China)

Abstract: Carbon (C) atoms can be replaced by other atoms in specifically designed spots to regulate the properties of graphene. This is established by introducing impurities such as B and N into graphene. The band gap can be opened while the Dirac cone shifts above or below the Fermi level. This behavior is the same as p-type or n-type doping in semiconductors. Electronic states are observed at the Fermi level, and the charges are transferred from the impurities to C or vice versa. The static dielectric function $\varepsilon_1(0)$ increases greatly, a new absorption peak appears in the low-energy region corresponding to visible light and the following energy. The decrease in plasma excitation due to the B or N doping results in a reduction of the number of peaks in the electron energy loss function. Only one obvious peak is observed at the same position as that of the highest peal of pristine graphene. The height of this peak increases significantly.

Key words: graphene, doping, the first principles study, electronic properties, optical properties

PACS: 73.20.-r (73.20.At, 73.20.Hb), 78.20.-e (78.20.Ci), 78.67.-n (78.67.Bf)

第一性原理计算硼和氮原子对石墨烯光电性能的调制

李佳斌, 刘红侠*, 吴 磊

(西安电子科技大学微电子学院 宽禁带半导体材料和器件重点实验室,陕西 西安 710071)

摘要:通过设计B和N原子取代碳原子,可以实现对石墨烯性能的调制.结果显示,石墨烯的带隙被打开,狄拉克锥在费米能级上上下移动,类似于对其进行p型或n型掺杂.在费米能级处电子态存在,电荷从杂质转移到C原子上或者从碳原子转移到杂质上.静态介电函数$\varepsilon_1(0)$增大,在对应可见光及其以下的能量区域出现了新的吸收峰.由于B或N的掺杂,使得石墨烯中等离子体激发减少,导致了电子能量损失函数峰值的减少.只有一个明显的峰值与本征石墨烯最高峰的位置相同,但是峰值的高度显著增加.

关 键 词:石墨烯;掺杂;第一性原理;电子性能;光学性能

中图分类号:O469　　**文献标识码**:A

Introduction

Graphene has attracted extensive interest in the wide scientific community for its outstanding physical and electronic properties. For its application in photoelectric devices, the semi-metallic nature of the zero band gap is an obstacle. Some methods have been taken to modulate the energy band of graphene, which contain quantum limiting effect[1-2], feet side effect, edge effect, doping effect[3], and introducing external field[4]. Furthermore, the absorptivity of a single layer graphene is only 2.3%, whereas in the visible region, the reflectivity of a single layer graphene is less than 0.1%. The optical performance of graphene is far from our expectation. Recently, some experimental and theoretical papers have shown that carbon atoms can be replaced with other atoms in specifically designed spots[5-6]. In the present study, the effect

Received date: 2017-09-04, **revised date**: 2017-12-15　　**收稿日期**:2017-09-04, **修回日期**:2017-12-15

Foundation items: Supported by the National Natural Science Foundation of China (61376099), the Foundation for Fundamental Research of China (JSZL2016110B003) and the Major Fundamental Research Program of Shaanxi (2017ZDJC-26)

Biography: LI Jia-Bin (1986-), male, Jiamusi, Heilongjiang province, master. Research area involves photoelectric properties of two-dimensional materials and Ⅲ-Ⅴ compounds. E-mail:15991730364@163.com

* **Corresponding author**: E-mail: hxliu@mail.xidian.edu.cn

of impurities on the photoelectric properties of the graphene were investigated by considering the case of boron (B) and nitrogen (N) doping, and the reasons for the changes in these properties were analyzed.

1 Computational method

First principles calculation is a common used computational method in the research field of new material such as ferroelectric materials[7], photoelectric materials[8], and two-dimensional materials[9]. In this paper, the CASTEP (Cambridge Sequential Total Energy Package) module is adopted, and simulations are performed under generalized gradient approximation (GGA) with Perdew-Burke-Ernzerhof (PBE) exchange and correlation. In the process of structure optimization, 500 eV mesh cutoff energy is set for the expansion of plane wave basis sets and the convergence criteria is set to 5×10^{-6} eV for all systems. The Brillouin-zone (BZ) integration is calculated by the highly symmetric K points in the form of a Monkhorst-Pack $7 \times 7 \times 1$ grid. The convergence criterion of the maximal displacement of atoms is 1×10^{-3} Å. The Bader charge analyzing is adopted to calculate the charge transfer ΔQ. All calculations are carried in reciprocal space with C: $2s^2 2p^2$, B: $2s^2 2p^1$, and N: $2s^2 2p^3$ as the valence electrons.

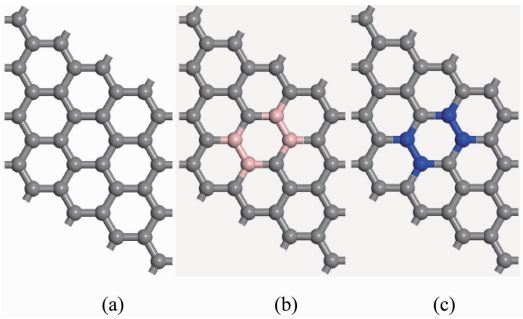

Fig. 1 Super cell of the graphene structures (a) pristine, (b) B doping, and (c) N doping. Blue balls represent N atoms, pink balls represent B atoms. The doping concentration is 12.5%

图1 石墨烯超原胞结构 (a)本征,(b) B 掺杂,(c) N 掺杂. 蓝色球代表 N 原子,粉色球代表 N 原子. 掺杂浓度为 12.5%

2 Results and discussion

2.1 Structures

Table 1 The variation of bond length and charge after optimizing

表1 优化后键长和电荷的变化

Structure	Bond length /nm			Number of charges	
	C-C	C-B	C-N	B	N
Pristine Graphene	0.142 1	–	–	–	–
Graphene doped with B	–	0.148 3	–	0.52	–
Graphene doped with N	–	–	0.139 6	–	-0.25

Figure 1 shows the structures of $4 \times 4 \times 1$ pristine graphene and graphene with B or N doping. A 15 Å vacuum region perpendicular to the graphene surface is added, which is verified to be wide enough. The constructed structures are optimized to achieve the steady state. Because of the difference in the radius of the atom, there is a change in the bond length after B and N doping as shown in Table 1. Compared with the C-C bond in the pristine graphene, the C-B bond in the graphene doped with B increased by 4.36%, while the C-N bond in the graphene doped with N shrunk by 1.76%. The results are similar to Ref. [10].

2.2 Electronic properties

Graphene has many interesting properties owing to its Dirac cone. The band structure of pristine graphene, exhibits a zero band gap with linear dispersion relation around E_F at K point in the brillouin zone, as is shown in Fig. 2(a). Figures 3(a) and (b) show the band structures of graphene doped with B and N (12.5% doped). The band gap of graphene increased to a certain degree owing to doping by B and N atoms. For the B-doped graphene, the band gap Eg is 0.64 eV, Dirac cone ascended above the Fermi level. This means that Fermi level lies in the valence band, which is the same as p-type doping. The results correspond to the Ref [11]. For the N-doped graphene, the band gap Eg is 0.6 eV, Dirac cone descended below the Fermi level. This indicates that Fermi level lies in the conduction band, which is the same as n-type doping. Eg is highly sensitive to the doping concentration of impurities. Figures 3(c) and (d) represent the band structures of graphene with different B and N doping concentration (50% doped). The band gap Eg increased, and the Dirac cone ascended or descended further relative to the Fermi level.

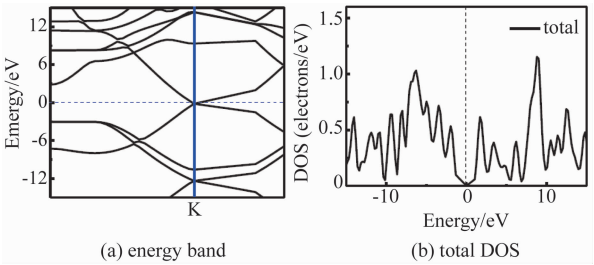

Fig. 2 Energy Band and total DOS of the pristine graphene. The blue solid lines represent K point, the dotted lines represent Fermi level

图2 本征石墨烯的能带结构和总的态密度. 蓝色的实线代表 K 点,虚线代表费米能级

Figure 2(b) represents the total DOS (density of states) of the pristine graphene. As seen from the figure, the conduction band and valence band met at Fermi level where the DOS was zero. Figures 4(a) and (b) represent the total DOS of the graphene doped with B and N. It can be seen that the electronic state of 0.9 eV^{-1} and 1.1 eV^{-1} were observed at the Fermi level; these values correspond to the interaction between the impurities and C atom. Figure 4 represents the PDOS (partial density of states) of graphene doped with B and N. In Fig. 5(a), the B $2p$ states lie below E_F have more electrons than the C $2p$ states of graphene, which indicates that charge transfer occurs from B atom to C atom; 0.52 electrons transfer from the $2p$ state of B to the $2p$ states of C ,

which is similar to the Ref [12]. In Fig. 5(b), the N 2*p* states lie above E_F have less electrons than the C 2*p* states of graphene, which means that charge transfer occurs from C atom to N atom; 0.25 electrons transfer from the 2*p* state of C to the 2*p* states of N.

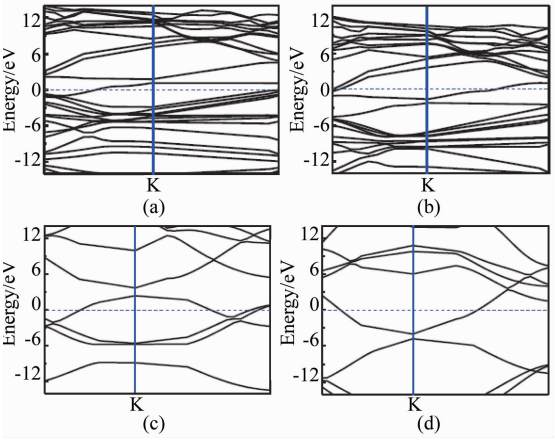

Fig. 3　Energy band of the doped structures of graphene with different doping concentration: (a) B doping (doping concentration is 12.5%), (b) N doping (doping concentration is 12.5%), (c) B doping (doping concentration is 50%), (d) N doping (doping concentration is 50%). The blue solid lines represent K point, the blue dotted lines represent Fermi level

图 3　掺杂石墨烯在不同掺杂浓度下的能带结构:(a) B 掺杂(掺杂浓度为 12.5%),(b) N 掺杂(掺杂浓度为 12.5%),(c) B 掺杂(掺杂浓度为 50%),(d) N 掺杂(掺杂浓度为 50%). 蓝色的实线代表 K 点,蓝色虚线代表费米能级

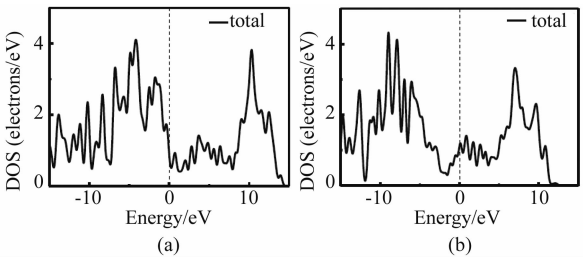

Fig. 4　Total DOS of the doped structures of graphene: (a) B doping, (b) N doping. The dotted lines represent Fermi level

图 4　掺杂石墨烯总的态密度:(a) B 掺杂,(b) N 掺杂. 虚线代表费米能级

2.3　Optical properties

The optical properties of photoelectric materials are mainly characterized by the dielectric function, optical absorption spectra, conductivity, loss function, refractive index and reflection coefficient. The optical constants, relating the microscopic model of physical process with the microelectronic structure of the solid that can better characterize the physical properties of the material, are mainly determined by the electronic structures and the carrier concentration near the Fermi level. The changes in the electronic structures of graphene caused by the doping of B and N would influence its optical properties. The optical properties of the three doping structures of graphene (pristine, B doping, and N doping) are depicted in Fig. 5, the doping concentration is 12.5%.

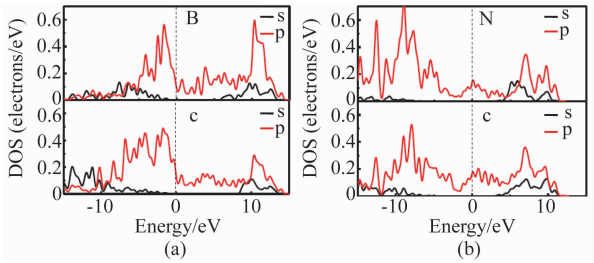

Fig. 5　PDOS of the doped structures of graphene: (a) B doping, (b) N doping. The dotted lines represent Fermi level

图 5　掺杂石墨烯结构的分波态密度:(a) B 掺杂,(b) N 掺杂. 虚线代表费米能级

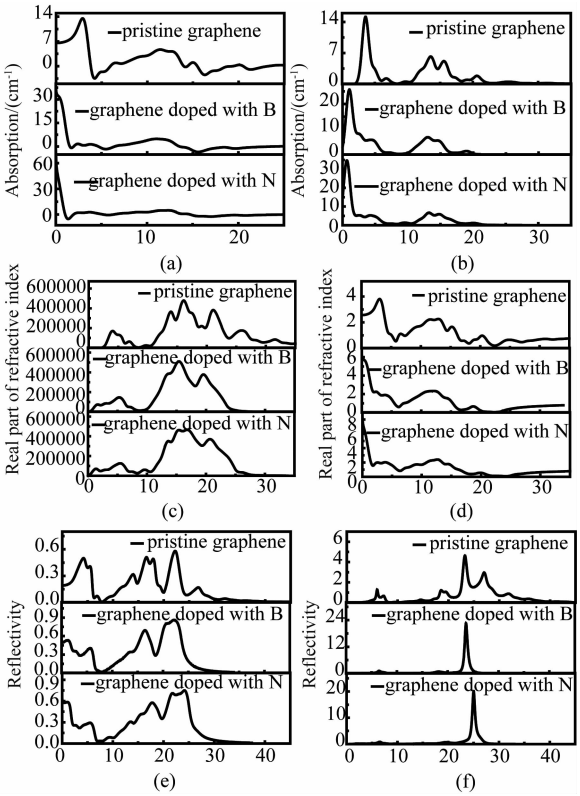

Fig. 6　Optical properties of pristine graphene and doped graphene (doping concentration is 12.5%): (a) Real part of dielectric function, (b) imaginary part of dielectric function, (c) absorption spectra, (d) real part of refractive index, (e) reflectivity, and (f) loss function

图 6　本征石墨烯和掺杂石墨烯(掺杂浓度为 12.5%)的光学性能:(a)介电函数的实部,(b)介电函数的虚部,(c)吸收谱,(d)折射率的实部,(e)反射率,(f)损失函数

2.3.1　Dielectric function and optical absorption

Within the linear response range, the structure of the energy band of a solid and other kinds of spectral information can be obtained from the dielectric function, which associates the micro-physical process of inter-band transition with the electronic structure of the solid. In the dielectric function, the decline of the real part determines the peak value of the imaginary part, and the imaginary part represents the optical absorption intensity.

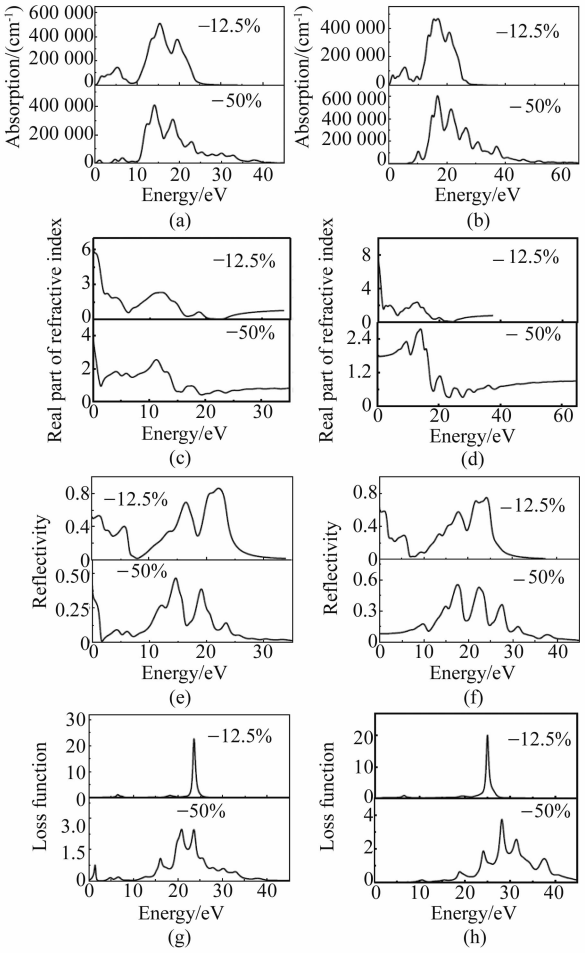

Fig. 7 Optical properties of the graphene with different doping atoms and concentration: (a) ~ (b) Absorption spectra of graphene doped with B and N, (c) ~ (d) real part of refractive index of graphene doped with B and N, (e) ~ (f) reflectivity of graphene doped with B and N, and (g) ~ (h) loss function of graphene doped with B and N

图7 不同掺杂原子和不同掺杂浓度石墨烯的光学性能(a)~(b)B 和 N 掺杂石墨烯的吸收谱,(c)~(d)B 和 N 掺杂石墨烯的折射率的实部,(e)~(f)B 和 N 掺杂石墨烯的反射率,(g)~(h)B 和 N 掺杂石墨烯的损失函数

Figures 6(a) and (b) represent the frequency-dependent real and imaginary parts of the dielectric function $\varepsilon(\omega)$ of the three different doping structures of graphene ($\varepsilon_1(\omega)$ represents the real part of the dielectric function, $\varepsilon_2(\omega)$ represents its imaginary part). For pristine graphene, the static dielectric function $\varepsilon_1(0)$ was 6.56, the maximum value of the real part was 13.51 at an optical energy of 2.90 eV, and the minimum value was found to be −3.47 at an optical energy of 4.22 eV. With an increase in the optical energy, the real part decreased rapidly in the range 2.90-4.22 eV, which indicates that the imaginary part increased rapidly in this range. However, fluctuation in the trend of the imaginary part were also observed at certain points over the whole optical energy range. The optical energy of the imaginary part was divided into two parts— 0-8.43 eV in the low region and 8.43-34 eV in the high region. The main peaks of $\varepsilon_2(\omega)$ in the different region correspond to the specific inter-band transition. Two main peaks in the low energy region were observed in the graph of $\varepsilon_2(\omega)$ at optical energies of 3.59 and 6.74 eV, which correspond to the transition σ -π *. Three main peaks in the high energy region were observed in the graph of $\varepsilon_2(\omega)$ at optical energies of 13.56, 15.56, and 20.63 eV, which correspond to the transition σ-σ *.

Figure 6(c) shows the absorption coefficients of the three different structures of graphene. For pristine graphene, the maximum absorption coefficient was 478 800 cm^{-1} at an optical energy of 16.11 eV in the high-energy region and the intensity of the absorption spectra in the absorption spectra was higher than that in the low-energy region. The absorption edge began at the optical energy of 1.24 eV, which corresponds to the transition threshold of σ-π *, but low absorption intensity was observed for the visible light (1.38 ~ 3.26 eV).

After the introduction of B and N impurities into graphene, the static dielectric function $\varepsilon_1(0)$ increased greatly, the intensity and the positions of the peaks of $\varepsilon_2(\omega)$ that represent the transition σ-σ * in the high energy region changed slightly. Meanwhile, the intensity of $\varepsilon_2(\omega)$ that represent the transition σ-π * in the low energy region increased and the positions of the peaks shifted to the lower region. The intensity and the positions of the absorption spectrum changed slightly, but the absorption spectrum shrunk considerably in the high-energy region. A new absorption peak appeared in the low-energy region containing the visible light and the following energy, which indicates that the absorption intensity of the visible light and the infrared increased greatly. This change is attributed mainly to the presence of B and N impurities enhance the electron-hole interaction and the impurity states, thus providing a competing path for optical excitation so that graphene doped with B and N contains electron-hole pairs that then form bound excitons (excitonic transition) enhancing the light absorption in the low energy region.

Different doping concentration of impurities affect the optical properties of graphene to different degrees. Figures 7(a) and (b) shows the absorption coefficients of graphene with different concentration of impurities. Significant shrinkage of the absorption spectrum in the low-energy region and broadening occurred in the high-energy region with the increase in doping concentration (50% doped). In the case of graphene doped with B, the maximum intensity of the peaks of the absorption spectrum decreased, small individual peaks occurred in the low-energy region. In the case of graphene doped with N, the maximum intensity of the peaks of the absorption spectrum increased, no peak was observed in the low-energy region.

2.3.2 Reflectivity and refractive index

The real part of the refractive index $n(\omega)$ is shown in Fig. 6(d). The static value of refractive index $n(0)$ of pristine graphene was 2.56, and the maximum value of its real part was 3.81 at an optical energy of 3.07 eV. The absorption of the high-frequency electromagnetic wave decreased with increase in the photon energy above 30 eV. The change in the refractive index was very small. In the case of graphene doped with B or N, the maximum value

of $n(\omega)$ increased, and the peak position shifted to the low-energy region accompanied by significant reduction in $n(\omega)$ in the high-energy region. Figures 7(c) and (d) show $n(\omega)$ of graphene with different concentration of impurities. The maximum value of $n(\omega)$ decreased greatly, and significant increase in the refractive index was observed in the high-energy region with increase in doping concentration (50% doped). In the case of graphene doped with B, a new peak appeared in the low-energy region. In the case of graphene doped with N, the position of the peak in the low-energy region shifted towards the high-energy region direction.

The optical parameter corresponding to the refractive index is reflectivity $R(\omega)$, which is shown in Fig. 6 (e). The maximum reflectivity of pristine graphene was 0.58 at an optical energy of 22.24 eV. The reflectivity observed at optical energies above 35 eV was very small. In the case of graphene doped with B or N, the maximum value of $R(\omega)$ increased, and the peaks in the low-energy region shifted toward further lower-energy region. In addition, the optical energy range decreased to values less than 30 eV. Figures 7(e) and (f) show $R(\omega)$ of graphene with different concentration of impurities. The maximum value of $R(\omega)$ decreased, and its position shifted toward further lower-energy region with increase in doping concentration (50% doped). Furthermore, the peaks in the low-energy region shifted toward the high energy region direction.

2.3.3 Electron energy loss function

The electron energy loss (EELS) function describes the energy loss of electrons in a homogeneous medium. The peak value of the function represents plasma turbulence, and the corresponding oscillation frequency is known as the plasma frequency. The EELS is shown in Fig. 6(f). Several peaks were observed, the maximum height of the peaks was 4.64 at an optical energy of 23.24 eV for pristine graphene. In the case of graphene doped with B or N, only one obvious peak was observed in the same position as the maximum height of pristine graphene, and the height of this peak increased significantly; the peak position corresponds to the edge energy of plasma and indicates the transition point from a semimetallic to semi-conductor material. This indicates that the presence of B or N in the graphene reduces plasma excitation in the low-energy region and part of high-energy region. The plasma excitation peaks increased, and the EELS peak broadened; the height of the peaks decreased significantly with increase in doping concentration (50% doped).

3 Conclusions

Based on the first principle density functional theory calculation, the electronic and optical properties of graphene doped with B and N are investigated in this study. The electronic and optical properties of graphene were regulated significantly by B or N doping. The band gap was opened and increased with an increased in doping concentration. Interaction between the impurities and C atom, causing charge transfer, were observed. The changes in the optical properties occurred mainly in the low-energy region, the curves of these parameters shrunk in the high-energy region. The peaks of the optical parameters in the low energy region shifted toward the high energy region with the increase in the doping concentration (50% doped), and the peaks of some parameters in the low-energy region disappeared, as seen from the EELS.

References

[1] WANG Xin-Ren, DAI Hong-Jie. Etching and narrowing of graphene from the edges [J]. Nature Chemistry. 2010, **2**: 661 - 665.

[2] JIAO Li-Ying, WANG Xin-Ran, Diankov G, *et al*. Facile synthesis of high-quality graphene nanoribbons [J]. Nature Nanotechnology. 2010, **5**:321 - 325.

[3] YUN Jiang-Ni, ZHANG Zhi-Yong, YAN Jun-Feng, *et al*. First-principles study of B or Al-Doping effect on the structural, electronic structure and magnetic properties of γ-graphene [J]. Computational Materials Science. 2015, **108**:147 - 152.

[4] ZHANG Yuan-Bo, TANG Tsung-Ta, Girit C, *et al*. Direct observation of a widely tunable bandgap in bilayer Graphene [J]. Nature, 2009, **459**: 820 - 823.

[5] Robertson A W, Montanari B, He K, *et al*. Dynamics of single Fe atoms in graphene vacancies[J]. Nano Letters. 2013, **13**(4):1468 - 1475.

[6] Crook C B, Constantin C, Ahmed T, *et al*. Proximity-induced magnetism in transition metal substituted graphene [J]. Scientific Reports. 2015, **5**:12322.

[7] Nossa J F, Naumov I I, Cohen R E. Effects of manganese addition on the electronic structure of BaTiO3 [J]. Physical Review B. 2015, **91** (21): 214105.

[8] JIA Yan-Jun, DU Yu-Jie, WANG Mei-Shan. First-principles studies of electronic structure and optical properties of GaN surface doped with Si [J]. Optik. 2014, **125**: 2234 - 2238.

[9] Ebnonnasir Abbas, Narayanan Badri, Kodambaka Suneel, *et al*. Tunable MoS2 bandgap in MoS2-graphene heterostructures [J]. APPLIED PHYSICS LETTERS. 2014, **105**: 031603.

[10] Panchakarla L S, Subrahmanyam K S, Saha S K, et al. Synthesis, structure, and properties of boron-and nitrogen-doped graphene [J]. Adv. Mater. 2009, **21**:4726.

[11] ZHANG Yun-Qiu, LIANG Yong-Ming, ZHOU Jian-Xin. Recent Progress of Graphene Doping [J]. Acta Chim. Sinica. 2014, V72(3): 367 - 377.

[12] SHENG Zhen-Hua, GAO Hong-Li, BAO Wen-Jing. Synthesis of boron doped graphene for oxygen reduction Reaction in fuel cells [J]. Mater. Chem. 2012, V22(2):390 - 395.

(上接第 24 页)

[15] Ma C, Huang Y, Duan X, *et al*. High-transmittivity non-periodic subwavelength high-contrast grating with large-angle beam-steering ability [J]. *Chinese Optics Letters*, 2014, **12**(12):120501 - 120501.

[16] fang w, Huang Y, Ma C, *et al*. *High-contrast-gratings reflector based on SOI with large-angle beam steering ability*: Asia Communications and Photonics Conference, Shanghai, 2014[C]. [*s. n.*]

[17] Fang W, Huang Y, Duan X, *et al*. Non-periodic high-index contrast gratings reflector with large-angle beam forming ability [J]. *Optics Communications*, 2016, **367**:6 - 11.

[18] Faez R, Marjani A, Marjani S. Design and simulation of a high power single mode 1550nm InGaAsP VCSELs [J]. *IEICE Electron Express*, 2011, **8**(13):1096 - 1101.

[19] Karagodsky V, Pesala B, Chase C, *et al*. Monolithically integrated multi-wavelength VCSEL arrays using high-contrast gratings [J]. *Optics Express*, 2010, **18**(2): 694 - 699.